

Antibody conjugated graphene nanocomposites for pathogen detection

Chandan Sign^{1,2}, Gajjala Sumana¹

¹ Biomedical Instrumentation Section, Materials Physics and Engineering Division, National Physical Laboratory, (Council of Scientific & Industrial Research), Dr. K. S. Krishnan Road, New Delhi-110012, India

² Academy of Scientific and Innovative Research (AcSIR), CSIR-National Physical Laboratory Campus, Dr. K. S. Krishnan Marg, New Delhi-110012, India

E-mail: chandan.jadaun@gmail.com, sumanagajjala@gmail.com

Abstract. Graphene oxide (GO), due to its excellent electrochemical properties and large surface area, known to be highly suitable material for biosensing application. Here, we report *in situ* synthesis of silver nanoparticles (AgNPs) onto the GO sheets for the electrochemical detection of *Salmonella typhimurium* (*S.typhimurium*). The GO-AgNPs composites have been deposited onto the indium tin oxide (ITO) coated glass substrate by the electrophoretic deposition technique. Carbodiimide coupling (EDC-NHS) has been used for the immobilization of antibodies of *Salmonella typhimurium* (anti-*S.typhimurium*) for detection of *S.typhimurium*. The electron microscopy and UV-visible studies reveal successful synthesis GO-AgNPs composites while FT-IR studies suggest the proper immobilization of anti-*S.typhi*. The cyclic voltammetry (CV) has been utilized for detection using anti-*S.typhi*/GOAgNPs/ ITO based immunoelectrode as a function of *S.typhimurium* concentration. The fabricated immunosensor shows improved sensitivity of 33.04 $\mu\text{ACFU}^{-1}\text{mLcm}^{-2}$ in a wide detection range of 10f to 10⁶ CFU^{mL}⁻¹. This immunosensor may be utilized for the detection of other food borne pathogens like aflatoxin and *E.coli* also.

1. Introduction

The ability to detect various types of pathogen present in food supply chain like production, packaging and the storage is very important in order ensures the food safety and good health [1]. There are number of food borne diseases cause by bacterial and viral infection occurs across the globe. Food borne illness is responsible for 76 million illness, 325,000 hospitalizations and thousands death annually across the globe [2]. Among various types of food borne pathogens, *S.typhimurium* is responsible for frequently occurring food borne illness. This pathogen infects various types of foods including chicken, ground beef, cucumber, and live poultry [3]. *S.typhimurium* is a gram-negative bacterium and origin of various types of illness including diarrhea, fever, and abdominal cramps [4]. It also generates localized infection in joints or even enters the human bloodstream. Several conventional methods have been developed for the detection of this toxic pathogen including specific agar media, to separate and count bacterial cells in particular sample. But these detection techniques take initially 3-4

¹ To whom any correspondence should be addressed.



days to generate the results and then further 6-7 days for the confirmation [5]. Since last two decades various electrochemical, electrical and optical detection methods have been reported for the detection of *S.typhimurium*. Among them electrochemical method found to be fast, reliable and affordable. Gehring *et al.* have reported the enzyme-linked immunomagnetic electrochemistry based technique for *S.typhimurium* detection [6]. Liebana *et al.* have developed the electrochemical detection technique based on a magneto-electrode [7]. These techniques suffers several limitations including sensitivity and the detection limit. In this regard application of graphene oxide based traducers for the detection of *S.typhimurium* may overcome these challenges.

Since the introduction, graphene is considered as a highly suitable material for the biosensing application [8]. It is known to be a single layer of sp² bonded carbon atoms and exhibits a honeycomb structure having number of interesting properties such as very high electron mobility, room temperature quantum Hall effect; tunable optical properties, excellent electrical conductivity and high mechanical strength may provide potential applications in electrochemical detection of various bioanalytes [9-11]. Number of functional groups available on the basal and edge plane makes graphene oxide as a suitable material for biomolecular attachment [12]. Introduction of metal nanoparticles in the GO is known to improve the surface to volume ratio of the composites resulting into the improved loading of the biomolecules. Nanoparticles in host GO matrix improve the mechanical, catalytic and the conduction properties [13]. In addition to this, nanoparticles also act as the spacer between the GO sheets preventing them from the agglomeration. Silver nanoparticles (AgNPs) decorated GO is found to be highly suitable material for optoelectronics, catalysis and electrochemical applications. Wan *et al.* has designed a GO-AgNPs based efficient electrochemical biosensor to detect the anti-sulfate reducing bacteria [14]. A sensitive detection of tryptophan has also been reported by using GO-AgNPs transducer matrix [15]. In the current manuscript we have reported the *in situ* reduction and decoration of AgNPs in the GO sheet. This nanocomposite has been further utilized for the detection of *S.typhimurium* using CV technique.

2. Materials and Methods

2.1. Chemicals

Graphite powder flakes (45 μ m, >99.99 wt %) were procured from Sigma Aldrich, USA. *S. typhimurium* antibody and antigens (heat killed *S. typhimurium* cells) were purchased from KPL Laboratory, USA. Bovine serum albumin (BSA), 1-ethyl-3-(3-dimethylaminopropyl) carbodiimide (EDC) and N-hydroxysuccinimide (NHS) were procured from Sigma, Aldrich, USA. Silver nitrate has been purchased from SD Fine Chem. Mumbai, India.

2.2. Characterization

The UV-visible spectroscopy (Perkin-Elmer, Lambda 950), Fourier transform infra-red spectroscopic (FT-IR, Perkin-Elmer, Model 2000) were used for characterization of the synthesized nanocomposite. The structural and morphological studies were carried out using scanning electron microscopy (SEM, LEO 440), transmission electron microscopy (TEM, Tecnaii-G2F30 STWIN). Electrochemical studies were performed on cyclic voltammetry conducted using Autolab, Potentiostat/Galvanostat (Eco Chemie, the Netherlands, Model AUT84275).

2.3. Methods

2.3.1. Synthesis of GO-AgNPs nanocomposite

Synthesis of GO has been achieved using the method reported in literature [16]. For the synthesis of GO-AgNPs, 1 ml of AgNO₃ (2 mM) has been added into the 10 mL of GO (1 mg/mL) kept in the smooth stirring with a temperature of 50°C for 30 min. Then, 2 mL of ascorbic acid (5mM) has been added into the solution and the temperature has been raised to 70 °C.

2.3.2. Electrophoretic deposition of GO-AgNPs on ITO electrode

Deposition of GO-AgNPs on the ITO electrode has been achieved using electrophoretic deposition (EPD) technique using two electrode systems. In details, using EPD setup 65V of DC voltage has been applied in the solution containing GO-AgNPs in the acetonitrile solution for 90 sec. In order to obtain a surface charge on the GO-AgNPs 10^{-5} to 10^{-4} mol of $\text{Mg}(\text{NO}_3)_2 \cdot 6\text{H}_2\text{O}$ is added into the suspension as an electrolyte for EPD as Mg^{2+} ions adsorbed by the GO sheets provide an adequate positive surface charge to the GO-AgNPs sheets, resulting in enhanced deposition rate at the ITO electrode [17].

2.3.3. Biofunctionalization of the GO-AgNPs nanocomposite

Immobilization of the *anti-S.typhimurium* has been performed using carbodimide coupling chemistry. Prior to the covalent immobilization process, the COOH groups available in the GO-AgNPs electrode is activated, using EDC as the coupling agent and NHS as activator. $10\ \mu\text{l}$ of *anti-S.typhimurium* dissolved in the phosphate buffer (pH 7.4) has been uniformly dispersed onto the GO-AgNPs electrode and kept in the humid chamber for 6 hr. This allows the development of the strong covalent bonding between the COOH groups of the GO-AgNPs and the amine group of the *anti-S.typhimurium*. In addition to this, strong electrostatic interaction between the negatively charged AgNPs and the positively charged groups present in *anti-S.typhimurium* may also results into the higher loading of the *anti-S.typhimurium*. BSA, solution (1mg/mL) is used to block the non-specific active sites of the *anti-S.typhimurium*/GO-AgNPs bioelectrode.

3. Results and discussions

3.1. UV-Visible spectroscopy analysis

Figure 1A shows the detailed investigation of aqueous suspensions GO, AgNPs and GO-AgNPs using UV-Vis in the range of 200-800 nm with a slit width of 2 nm. The GO shows the peak at 231 nm mainly due to the $\pi - \pi^*$ transition of the various C-C bonds present in the GO. However, the composite shows a strong peak at 442 nm representing the significant number of AgNPs present in the nanocomposite. Another significant peak was found to be at 219 nm that may represent the blue shifting of the GO peak due to the introduction AgNPs. This phenomenon may occur due to the close conjugation of GO and the AgNPs resulting into the rapid electron transfer and increased transfer energy as reported in various literatures [18,19].

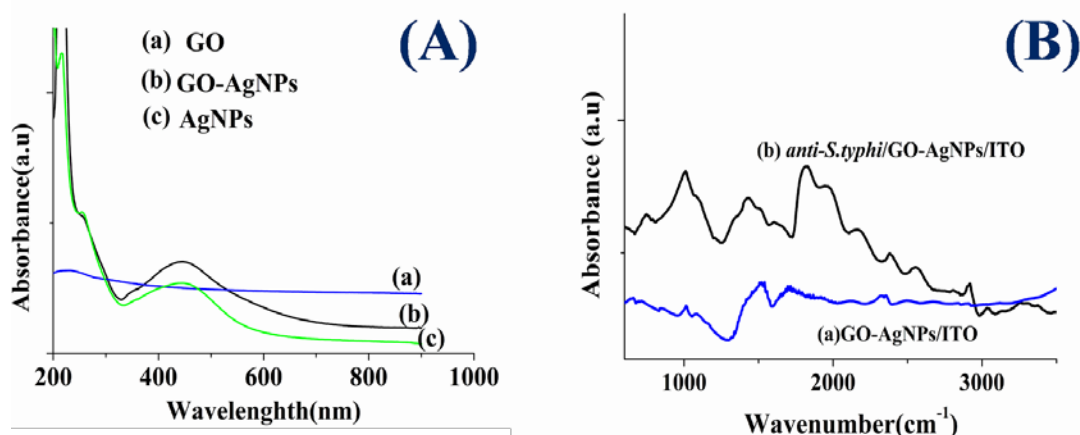


Figure 1. UV-visible studies of GO, AgNPs and GO-AgNPs (a), FTIR analysis of GO-AgNPs/ITO and *anti-S.typhimurium*/GO-AgNPs/ITO.

3.2. Furier Transform Infrared (FT-IR) spectroscopy analysis

FT-IR spectra of GO-AgNPs/ITO) and *anti-S.typhimurium*/GO-AgNPs/ITO films are shown in Figure

1B. The spectrum obtained for GO-AgNPs/ITO film shows a strong peak at 1598 cm^{-1} may be attributed to the stretching vibrations of C=C, the peak seen at 1297 cm^{-1} is due to C-O stretching. In the curve (b) strong peak at 1575 cm^{-1} represents the amide I bonding while the stretching, peak at 1256 cm^{-1} shows the C-O stretching and bending in the region of $3000\text{--}3500\text{ cm}^{-1}$ denotes primary and secondary amines representing the immobilization of *anti-S.typhimurium*.

3.3. Morphological Analysis

Figure 2 shows TEM images of the synthesized GO and the GO-AgNPs composites. Image (2A) shows the GO having various wrinkles and folding, while the image (2B) shows the AgNPs entirely distributed onto the GO sheets. The AgNPs, having different shape and size distributed on the GO sheet while, the AgNPs were in size range of 10-50 nm.

SEM investigation of GO-AgNPs and *anti-S.typhimurium*/GO-AgNPs/ITO immunoelectrode has been performed to get the surface characteristics of the synthesized materials (Fig. 3). Several agglomeration of the composite has been observed that may be due to the application of the high DC voltage for the fabrication of the film. Figure 3B shows the magnified small region on the GO-AgNPs as various layers of the GO composite with agglomerated AgNPs, are clearly visible. Figure 3C shows the EDX spectrum of the region shown in the image (3B). The GO-AgNPs composites have significant amount of AgNPs as shown in the image. After the immobilization of *anti-S.typhimurium* the GO-AgNPs/ITO, shows the uniform coverage of the biomolecule (Image 3D). This may be due to the strong interaction between the *anti-S.typhimurium* and the GO-AgNPs composites.

3.4. Electrochemical characterization studies

Electrochemical characterization of the GO-AgNPs and *anti-S.typhimurium*/GO-AgNPs immune electrode has been performed using CV (Figure 4A). The GO-AgNPs shows the anodic peak current of $322.2\mu\text{A}$ as shown in the curve (a). The higher amount of current may be due to AgNPs, as they offer the addition channels for the electron transport. But the *anti-S.typhimurium*/GO-AgNPs/ITO shows relatively lower value of the anodic peak current ($212.04\mu\text{A}$), as the immobilized biomolecules shows the insulation nature resulting into the blockage of the electron transport pathways.

The CV response of the *anti-S.typhimurium*/GO-AgNPs/ITO immunoelectrode as a function of scan rate ($10\text{--}100\text{ mVsec}^{-1}$) has been shown in the Figure 4B. It has been observed that the value of both anodic and cathodic peak current has been increases as a function of the square root of the scan rate indicating that redox reaction is controlled by semi-infinite linear diffusion process leading to the improved electron transfer kinetics. The slopes and the intercept are given by the following Eq. (1) and (2).

$$I_a[A] = 0.58 \times 10^{-6}[A] + 29.5 \times 10^{-6}[A^2s/mV]^{1/2} \times [\text{scanrate}(\frac{mV}{s})]^{1/2}; R^2=0.99 \quad (1)$$

$$I_c[A] = -34.55 \times 10^{-6}[A] - 19.60 \times 10^{-6}[A^2s/mV]^{1/2} \times [\text{scanrate}(\frac{mV}{s})]^{1/2}; R^2=0.99 \quad (2)$$

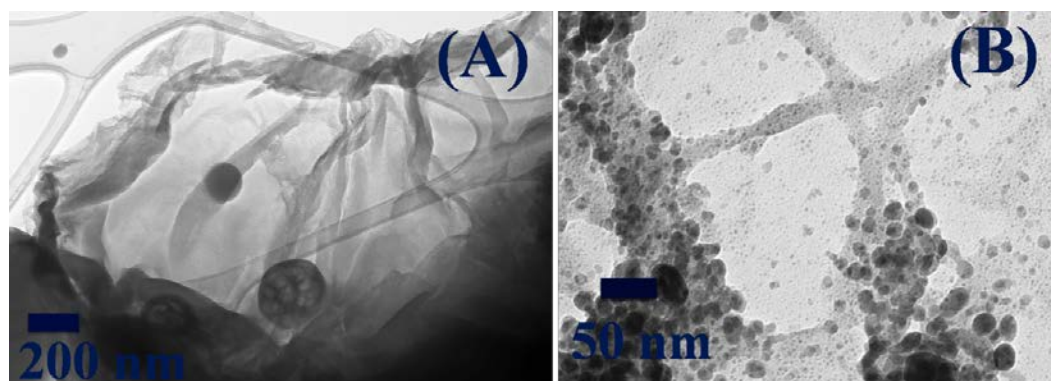


Figure 2. TEM image of synthesized GO (A), and GO-AgNPs nanocomposites (B)

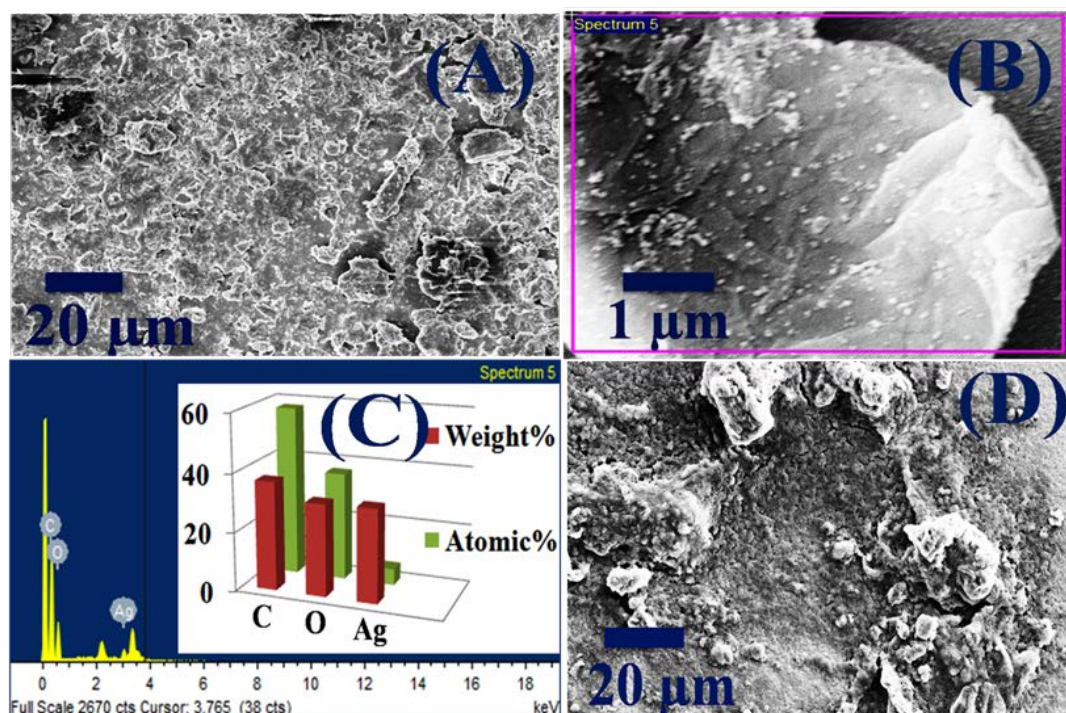


Figure 3. SEM image of GO-AgNPs/ITO (A), magnified region of GO-AgNPs/ITO (B) EDX spectrum of GO-AgNPs/ITO (C) and, *anti-S.typhimurium*/GO-AgNPs/ITO (D).

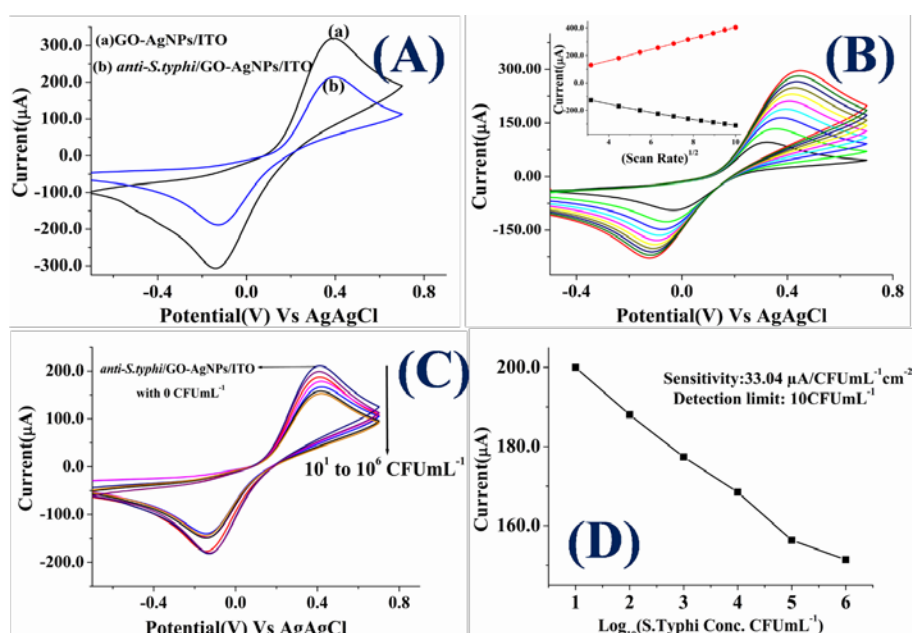


Figure 4. Electrochemical characterization of GO-AgNPs/ITO and *anti-S.typhimurium*/GO-AgNPs/ITO (A), Scan rate studies of *anti-S.typhimurium*/GO-AgNPs/ITO immunoelectrodes (B), Electrochemical response studies of *anti-S.typhimurium*/GO-AgNPs/ITO immunoelectrode as a function of *S.typhimurium* concentration (C), and Calibration plot obtained using *anti-S.typhimurium*/GO-AgNPs/ITO using different concentration of *S.typhimurium* (D).

3.5. Electrochemical response studies

Electrochemical response studies of anti-*S.typhimurium*/GO-AgNPs/ITO immunoelectrode has been performed as a function of *S.typhimurium* concentration (10^1 to 10^6 CFU/mL) using CV as shown in Figure 4C. It has been observed that the anodic peak current decreases as we increase the concentration of *S.typhimurium*. It may be due to the formation of the insulating antigen-antibody complex on the anti-*S.typhimurium*/GO-AgNPs/ITO immunoelectrode creating a barrier in the electron transport. As the concentration of the *S.typhimurium* increases the resistance gets increases in the same proportion. The calibration plot obtained between anodic peak current and *S.typhimurium* concentration has been shown in the Figure 4D. The fabricated immunosensor shows the high sensitivity of $33.04 \mu\text{A}/\text{CFU}^{-1}\text{mLcm}^{-2}$ and the lower detection limit of 10 CFU mL^{-1} . The higher loading of anti-*S.typhimurium* through the strong amide linkage and the electrostatic interaction with the composite may results into the strong signals. Superior loading of the anti-*S.typhimurium* using the carbodimide coupling may have resulted in the capturing of the higher number of incoming *S.typhimurium* cells. In addition to this AgNPs present on the surface of GO may have offers additional sites for the loading of anti-*S.typhimurium* by as electrostatic interaction between the negatively charged AgNPs and the positively charged amine ($-\text{NH}_2$) group available in the anti-*S.typhimurium*.

The designed immunosensor did not show any significance interference in the presence of other potential pathogens like *E.coli*. As shown in the Figure 5A only a negligible change (2.8%) in the current value has been observed, when *E.coli* has been added into the *S.typhimurium* (10^4 CFU mL^{-1}). In addition to this the anti-*S.typhimurium*/GO-Ag/ITO immunosensor found to be reproducible as shown in Figure 5B. Six different anti-*S.typhimurium*/GO-AgNPs/ITO immunoelectrode using 10^4 CFU mL^{-1} of *S.typhimurium* concentration shows almost same current. These immunoelectrodes has been prepared under the same condition and did not shows any significant change in the current value. The mean value has been calculated as $168.2 \mu\text{A}$.

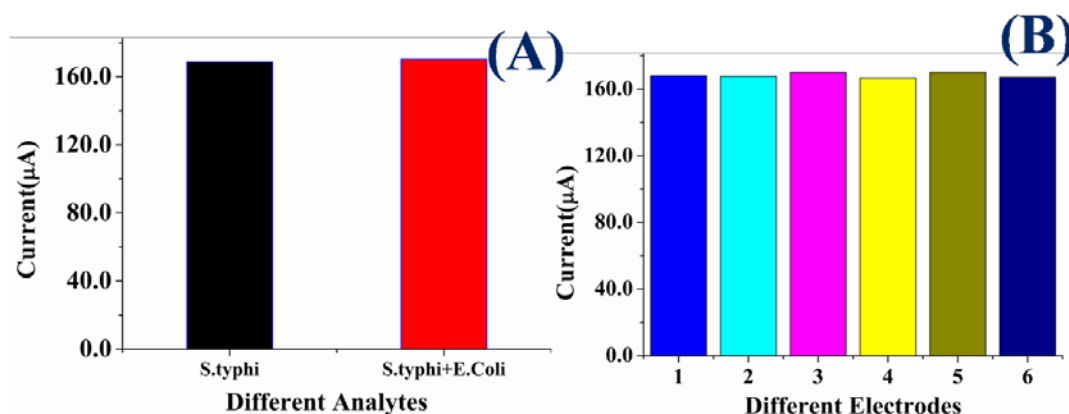


Figure 5. Interference study of anti-*S.typhimurium*/GO-AgNPs/ITO immunosensor (A), repeatability studies of anti-*S.typhimurium*/GO-AgNPs/ITO (B).

4. Conclusion

The GO-AgNPs based electrochemical immunosensor for *S.typhimurium* detection has been investigated in the present manuscript. A natural green and eco friendly route has been developed for the synthesis of GO-AgNPs using ascorbic acid. A well dispersed GO-AgNPs in acetonitrile has been utilized for the electrophoretic deposition and further EDC-NHS chemistry has been used to attach anti-*S.typhimurium*. Electron microscopy, and UV studies reveal successful synthesis of GO-AgNPs whereas FT-IR studies suggest its proper functionalized with anti-*S.typhimurium*. The fabricated immunosensor found to be efficient for the detection of *S.typhimurium* and may be utilized for other water and food borne pathogens.

Acknowledgement

We are highly thankful to Director, CSIR-National Physical Laboratory, New Delhi, India for providing the facilities. Chandan Singh is thankful CSIR, India for providing financial support as Senior Research Fellowship. Authors are thankful to Mr. Dinesh Singh and Jai Talwade for TEM and SEM investigations respectively. Authors are also thankful to Mr. Manoj Kumar Pandey for the technical support. Financial support received from the ESC-0103 is highly acknowledged.

Reference

- [1] Chai Y, Li S, Horikawa, S, Park M K, Vodyanoy V, and Chin B A 2012, *J. Food Prot.* , **75**, 631
- [2] Guntupalli R, Lakshmanan R S, Johnson M L, Hu J, Huang T S, Barbaree J M, and Chin B A, 2007, *Sens Instrum Food QualSaf*, **1**, 3
- [3] Onoda Ghosh D S, Barizuddin S, Yuksek N S, Dweik M, and Almasri M F, 2015. *J. Sens.* <http://dx.doi.org/10.1155/2015/293461>
- [4] Scharff R L, 2012. *J. Food Prot.*, **75**, 123
- [5] United States Department of Agriculture, Fact Sheets: Foodborne Illness and Disease, 2011, http://www.fsis.usda.gov/wps/portal/fsis/topics/food-safety-education/get-answers/foodsafety-fact-sheets/foodborne-illness-and-disease/salmonella-questions-and-answers/ct_index.
- [6] Gehring A G, Crawford C G, Mazenko R S, Van Houten L J, and Brewster J D. 1996, *J. Immunol. Methods*, **195**, 15
- [7] Liébana S., Lermo A, Campoy S, Cortés M P, Alegret S, and Pividori M I, 2009. *Biosens. Bioelectron.*, **25**, 510.
- [8] Kim J, Kim F, and Huang J., 2010, *Mater. Today*, **13**, 28
- [9] Huang X, Yin Z, Wu S, Qi X, He Q, Zhang Q, and Zhang H. 2011, *Small*, **7**, 1876
- [10] Wassei J K, and Kaner R B, 2010, *Mater. Today*, **13**, 52
- [11] Huang Y, Dong X, Shi Y, Li C M, Li L J, and Chen P, 2010 *Nanoscale*, **2**, 1485
- [12] Srivastava S, Kumar V, Ali, M A, Solanki P R, Srivastava A, Sumana G, and Malhotra B D, 2013, *Nanoscale*, **5**, 3043
- [13] Dhand V, Kyong Y R, Hyun J K, and Dong H J, 2013, *J. Nanomater.* **2013**, 158
- [14] Wan Yi, Yi W, Jiajia W, and Dun Z, 2010, *Anal. Chem.* **83**, 648
- [15] Li J, Daizhi K, Yonglan F, Fuxing Z, Zhifeng X, Mengqin L, and Deping W, 2013, *Biosens. Bioelectron.* **42**, 198
- [16] Marcano D C, Kosynkin D V, Berlin J M, Sinitskii A, Sun Z, Slesarev A, and Tour J M, 2010, *ACS Nano*, **4**, 4806
- [17] Singh C, Srivastava S, Ali M A, Gupta T K, Sumana G, Srivastava A, and Malhotra B D, 2013, *Sens. Actuators, B*, **185**, 258
- [18] Zhong L, and Kyusik Y, *Int. J. Nanomed.* **10**, 79
- [19] Sahu S R, Mayanglambam M D, Puspall M, Pratik S, and Krishanu B. 2013, *J. Nanomater.*, **6**, 65